IEEE Access
Multidisciplinary | Rapid Review | Open Access Journal

Received June 11, 2019, accepted July 21, 2019, date of publication July 25, 2019, date of current version August 9, 2019.

Digital Object Identifier 10.1109/ACCESS.2019.2930963

Design and Implementation of an Efficient Tracking Differentiator

YUNDE XIE[1], HEHONG ZHANG[2,3,4], (Student Member, IEEE), LONGHUA SHE[1], GAOXI XIAO[3,4], (Senior Member, IEEE), CHAO ZHAI[3,4], (Member, IEEE), AND TSO-CHIEN PAN[5]

[1]Beijing Maglev Transportation Development Company Ltd., Beijing 10024, China
[2]Interdisciplinary Graduate School, Nanyang Technological University, Singapore 637371
[3]Future ResilientSystems, Singapore-ETH Centre, Singapore 138602
[4]School of Electrical and Electronic Engineering, Nanyang Technological University, Singapore 639798
[5]Institute of Catastrophe Risk Management, Nanyang Technological University, Singapore 639798

Corresponding author: Hehong Zhang (hzhang030@e.ntu.edu.sg)

This work was supported in part by the National Research Foundation of Singapore (NRF) under its Campus for Research Excellence and Technological Enterprise (CREATE) program, in part by the Ministry of Education (MOE), Singapore, under Contract MOE 2016-T2-1-119, in part by the Interdisciplinary Graduate School, Nanyang Technological University, Singapore, and in part by the National Key Research and Development Program of China under Grant 2016YFB1200600.

ABSTRACT Differential signals play significant roles in control practices, but they are prone to noise corruption. A noise-tolerant time-optimal system-based tracking differentiator (TD) was first proposed by Jingqing Han, which is constructed in the form of state feedback control for a discrete-time and double-integral system. However, its performances of signal-tracking filtering and differentiation extraction are sensitive to the sampling period. To relax the sensitivity on the sampling period, a time-criterion-based feedback control algorithm is proposed to construct the TD. The control algorithm is derived by comparing the time that the initial state is driven to the switching curve or the origin with any given sampling period. The impact of the algorithm parameter setting on filtering is analyzed in the frequency domain. Meanwhile, a compensation scheme is introduced to deal with the trade-off between the filtering ability and phase delay. The simulation results show that the proposed TD has smaller static errors in signal-tracking filtering, and better differentiation acquisition compared with others. The experiments conducted on STM32F405 reveal that the proposed TD uses the shortest execution time among others for processing the same input signals.

INDEX TERMS Tracking differentiator, discrete time, time criterion, filtering, differentiation, phase delay compensation.

I. INTRODUCTION

The differentiation of a given signal in real time is a well-known yet challenging problem in control theory and engineering [1], [2]. For example, the proportional-integral-derivative (PID) control law developed in the last century still plays an essential role in modern control-engineering practices [3], [4]. Therein, the derivative control mode gives the controller an additional control action when the error changes consistently. However, derivative signals are prone to noise corruption and the derivative controls usually cannot be effectively implemented [5], [6]. For this reason, great efforts have been devoted to designing new differentiators, such as high-gain observer-based differentiator [7], linear time-derivative tracker [8], super-twisting second-order sliding-mode algorithm [9], robust exact differentiator [10], and finite time-convergent differentiator [11], [12] among others [13]- [15].

Initially proposed by Han [16], [17], the discrete-time optimal control based tracking differentiator (TD) with the noise-tolerant characteristic has widely used in filtering and differentiation acquisition [16]. The advantage of this TD is that it sets a weak condition on the stability of the systems to be constructed for TD and requires a weak condition on the input. In addition, it has advantageous smoothness compared with the sliding-mode-based differentiators encountered with the chattering problem [18]. Han used this TD as an important part of his active disturbance rejection control (ADRC) [19]. He also presented a nonlinear PID control based on this TD [20]. Therein, the TD acts not only as the derivative

The associate editor coordinating the review of this manuscript and approving it for publication was Mou Chen.

extraction, but also as a transient profile that the output of a plant could reasonably follow to avoid the setpoint jump in PID.

It is well known that the continuous-time time-optimal solution, i.e., bang-bang control, could incur considerable numerical errors in a discrete-time implementation [16]. To address this difficulty and construct a discrete-time TD, a discrete-time solution (denoted as *Fhan*) for a discrete double integral system was proposed by Han [16]. This control algorithm *Fhan* is determined by comparing the location of the initial state with the isochronic region that has to be obtained through a complicated non-linear boundary transformation [21]. For a discrete double integral system, driving a state point on the phase plane to the origin by using the *Fhan* algorithm, its state trajectory is suboptimal [21]. A bigger sampling period that may be needed in some engineering scenarios may result in bigger static errors or overshoots in signal tracking and differentiation extraction, which means that, in order to make Han's TD highly accurate in signal-tracking and differentiation extraction, one has to impose strict constraints on the sampling period.

To relax this particular constraint and improve performances in signal-tracking and differentiation extraction, an efficient time-criterion based control algorithm is proposed in this paper to construct the TD. Since the proposed algorithm is determined by comparing the time that the initial state sequence is driven to the switching curve or the origin with any given sampling period (the reason why we term it as via time criterion), it relaxes the strict constraint on selecting a proper sampling period for the proposed algorithm under different engineering scenarios.

The rest of the paper is organized as follows: the problem and the objective are explained in Section II. The time-criterion based feedback control algorithm and its corresponding TD are presented in Section III. The filtering ability analysis and a phase delay compensation scheme are given in Section IV. In Section V, simulation results among different differentiators on signal-tracking filtering, differentiation exaction and algorithm execution time (based on STM32F405) are demonstrated. Section VI concludes the paper.

II. PROBLEM STATEMENT

To construct a TD, the first procedure is to determine a control algorithm for a double-integral system that is described by [16]

$$\begin{cases} \dot{x}_1 = x_2, \\ \dot{x}_2 = u, \quad |u| \le r, \end{cases}$$

where r is a constant constraint of the control input. The resulting feedback control algorithm that drives the state from any initial point to the origin in the shortest time is

$$u = -rsign(x_1 - v + \frac{x_2|x_2|}{2r})$$

where v is the desired value for x_1. $\Gamma(x_1, x_2) = x_1 + \frac{x_2|x_2|}{2r}$ is the switching curve [22], [23]. Using this principle, one can construct the corresponding TD, that is, obtaining the desired trajectory and its derivative by solving the following differential equations:

$$\begin{cases} \dot{v}_1 = v_2, \\ \dot{v}_2 = -rsign(v_1 - v + \frac{v_2|v_2|}{2r}) \end{cases}$$

where v_1 is the desired trajectory, and v_2 is its derivative [16]. Based on the analysis above, the main procedure to construct the TD is to derive an efficient control algorithm for a double-integral system. Then, it can be easily extended to handle the tracking problem by replacing the first state variable x_1 with $x_1 - v$, where v is the desired value of x_1.

Consider a standard discrete-time double-integral system that is described by:

$$x(k+1) = Ax(k) + Bu(k), \quad |u(k)| \le 1 \tag{1}$$

where $A = \begin{bmatrix} 1 & h \\ 0 & 1 \end{bmatrix}$, $B = \begin{bmatrix} 0 \\ h \end{bmatrix}$, h is the sampling period. The objective is to design a feedback control algorithm (denoted as *Ftd*) for system (1) such that the state $x(k)$ is driven back to the origin in a finite number of steps. In order to relax the particular constraint on the sampling period for *Fhan* based TD, the control signal sequence in *Ftd*, i.e., $u(0)$, $u(1)$, ..., $u(k)$ is determined by comparing the time that the initial state point is driven back to the switching curve or the origin with any given sampling period h.

The time that any initial state point $M(x_{10}, x_{20})$ is driven back to the switching curve, i.e., $\Gamma(x_1, x_2) = x_1 + \frac{x_2|x_2|}{2}$, is denoted as t_A, and the time that the state point located on the switching curve is driven back to the origin is denoted as t_B. We can determine that $t_A = sx_{20} + \sqrt{sx_{10} + \frac{1}{2}x_{20}^2}$ and $t_B = |x_{20}|$, where $s = sign(x_{10}) + \frac{1}{2}x_{20}|x_{20}|$). The work of identifying the control signal sequence that drives any initial state to the origin can be divided into the following two tasks:

Task 1: Determine the control signal sequence when the initial state point $M(x_{10}, x_{20})$ is not located on the switching curve by comparing time t_A with the sampling period h.

Task 2: Determine the control signal sequence when the state point $M(x_{10}, x_{20})$ is located on the switching curve by comparing time t_B with the sampling period h.

III. ALGORITHM CONSTRUCTION

By fulfilling the above mentioned tasks, for any $M(x_{10}, x_{20})$, we have the corresponding feedback control algorithm for system (1). This is denoted as $u(k) = Ftd(x_1(k), x_2(k), r, h)$, where the parameter r is a constant constraint of the control input. Note that, since system (1) is a standard discrete-time double-integral system, there exists $r = 1$. To clearly present the algorithm, we list the satisfying conditions for any initial

state point $M(x_{10}, x_{20})$ as follows:

$$\begin{cases} \Omega_1 = \{(x_{10}, x_{20}) | x_{10} + \dfrac{x_{20}|x_{20}|}{2} > 0\} \\ \Omega_2 = \{(x_{10}, x_{20}) | x_{10} + \dfrac{x_{20}|x_{20}|}{2} < 0\} \\ \Omega_3 = \{(x_{10}, x_{20}) | x_{10} + \dfrac{x_{20}|x_{20}|}{2} = 0\} \end{cases}$$

The resulting control algorithm is

$$u(k) = \begin{cases} -s, \ if \ M \in \Omega_1 \cup \Omega_2, & h \le t_A \\ \dfrac{1}{2} - \dfrac{1}{h}x_{20} - \dfrac{1}{2}\sqrt{1 + \dfrac{4}{h}x_{20} + \dfrac{8}{h^2}x_{10}} & \\ \qquad\qquad if \ M \in \Omega_1, & h > t_A \\ -\dfrac{1}{2} - \dfrac{1}{h}x_{20} + \dfrac{1}{2}\sqrt{1 - \dfrac{4}{h}x_{20} - \dfrac{8}{h^2}x_{10}} & \\ \qquad\qquad if \ M \in \Omega_2, & h > t_A \\ -sign(x_{20}), & if \ M \in \Omega_3, \ h \le t_B \\ \dfrac{6}{h^2}x_{10} + \dfrac{2}{h}x_{20}, & if \ M \in \Omega_3, \ h > t_B \end{cases} \quad (2)$$

where $s = sign(x_{10} + \frac{1}{2}x_{20}|x_{20}|)$, $t_A = sx_{20} + \sqrt{sx_{10} + \frac{1}{2}x_{20}^2}$ and $t_B = |x_{20}|$. The detailed deduction of the control algorithm *Ftd* is given in Appendix A.

The proof that the proposed control input fulfills the given constraint, i.e, $|u(k)| \le 1$ in system (1) shall then be presented. The main result is the Theorem 1 below. Note that, when the state point $M(x_{10}, x_{20})$ is located on the switching curve, i.e, $\Gamma(x_{10}, x_{20}) = 0$, the control input satisfies the constraint apparently since $h > t_B = |x_{20}|$. Hence, we only need to prove that the control input fulfills $|u(k)| \le 1$ when the state point $M(x_{10}, x_{20})$ is not located on the switching curve.

Theorem: The control law $u(k)$ in (2) satisfies the condition $|u(k)| \le 1$.

Proof: See Appendix B.

The control algorithm in (2) can be easily extended to the tracking problem by replacing $x_1(k)$ in (1) with $x_1(k) - v$ and we can then construct the following TD:

$$\begin{cases} u(k) = Ftd(x_1(k) - v(k), c_1 x_2(k), r_0, c_0 h) \\ x_1(k+1) = x_1(k) + h x_2(k) \\ x_2(k+1) = x_2(k) + u(k)h \end{cases} \quad (3)$$

where v is the given signal, c_1 is the damping factor, r_0 is the quickness factor, c_0 is the filtering factor and h is any given sampling period. The filtering factor is of high importance in signal-tracking filtering performance.

Remark 1: Determined by comparing the time that the initial state point is driven back to the switching curve or the origin with any given sampling period h, the control algorithm *Ftd* that is used to construct the TD relaxes the strict constraint on the sampling period for the existing TD. For a general discrete-time double-integral system, its control algorithm *Ftd* can be derived by substituting x_1 and x_2 with z_1 and z_2, respectively, where $z_1 = \frac{x_1}{r}$ and $z_2 = \frac{x_2}{r}$. Meanwhile, $t_A = sx_{20}/r + \sqrt{sx_{10}/r + \frac{1}{2r^2}x_{20}^2}$ and $t_B = |x_{20}|/r$.

IV. STRUCTURE ANALYSIS AND PHASE DELAY COMPENSATION

A. STRUCTURE ANALYSIS

For a given signal sequence $v(k)(k = 0, 1, 2, \ldots)$, the discrete-time TD in (3) can be approximately transformed into a linear format as presented below by taking on the proper parameter r_0 (the quickness factor):

$$x(k+1) = Gx(k) + Hv(k), \quad k = 0, 1, 2 \ldots \quad (4)$$

where $x(k) = [x_1(k), x_2(k)]^T$ and $H = [\frac{1}{c_0^2}, \frac{2}{c_0^2 h}]^T$. $G = [G_1, G_2]^T$ where $G_1 = [1 - \frac{1}{c_0^2}, (1 - \frac{c_1}{c_0^2})h]$ and $G_2 = [-\frac{2}{c_0^2 h}, 1 - \frac{2c_1}{c_0}]$.

We assume that the given signal is $v(t) = \sum_{i=1}^{N} A_i e^{j(w_i t + \phi_{i0})} + \xi(t)$, where $\xi(t)$ is a width-steady process. Then we have

$$x(k) = G^k p_0 + \sum_{i=1}^{N} (e^{jw_i h} I_2 - G)^{-1} H A_i e^{j(w_i kh + \phi_{i0})} + \eta(k), \quad (5)$$

where $\eta(k+1) = G\eta(k) + H\xi(k)$, $k = 0, 1, 2, \ldots$, and p_0 is determined based on initial conditions $x(0)$ and $\eta(0)$. If the convergence of (5) is sufficient and necessary, then the spectral radius of matrix G satisfies $\rho(G) < 1$. Hence, $x_1(k) = CG^k p_0 + \sum_{i=1}^{N} C(e^{jw_i h} I_2 - G)^{-1} H A_i e^{j(w_i kh + \phi_{i0})} + C\eta(k)$ by choosing $C = [1, 0]$. When the transfer function of the discrete-time system is denoted as $\Phi(z) = C(zI_2 - G)^{-1}H$, $x_1(k)$ can be expressed as follows:

$$x_1(k) = CG^k p_0 + \sum_{i=1}^{N} \Phi(e^{jw_i h}) A_i e^{j(w_i kh + \phi_{i0})} + C\eta(k). \quad (6)$$

The characteristics of magnitude frequency and phase frequency for the TD in (3) are analyzed as follows. Given a sine signal $v(t) = Ae^{j(wt + \phi_0)}$, the tracking output signal y_{out} is also a sine signal when the particular signal sequence is long enough and the spectral radius of matrix G satisfies $\rho(G) < 1$. We suppose that the output signal is $y_{out} = \beta v(t - \tau_0)$, where β is the dynamic amplifier factor and τ_0 is the time delay. By choosing the filtering factor c_0 that satisfies condition $c_0 wh \ll 1$, we have

$$\begin{cases} \beta = \dfrac{1}{1 + 0.5c_0^2(c_1^2 - 1)w^2h^2} \\ \tau_0 = (c_0 c_1 - 1)h \end{cases} \quad (7)$$

Furthermore, when the damping factor $c_1 = 1$, we have $\beta = 1$ and $\tau_0 = (c_0 - 1)h$. Based on the conditions above, the characteristics of magnitude frequency and phase frequency are shown in Fig. 1, which illustrates that the filtering ability performs better as the filtering factor c_0 increases. However, the phase delay will increase in the proposed TD as the filtering factor c_0 increases.

The filtering characteristics are compared between *Ftd* based TD and *Fhan* based TD. Here, we consider only the width-steady random process. For a discrete-time linear-TD, the width-steady input leads to the width-steady output.

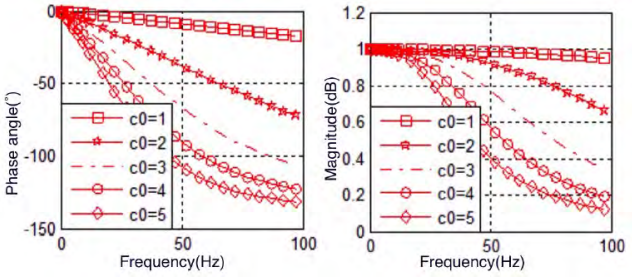

FIGURE 1. Characteristic curves of magnitude frequency and phase frequency for *Ftd* based TD.

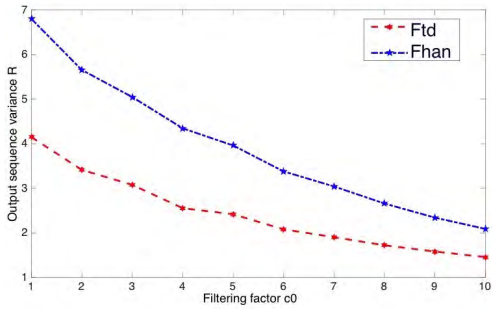

FIGURE 2. Output sequence variance R vs filtering factor c_0 for two algorithms.

When the random input sequence $\xi(t)$ is a white noise sequence, $R_\xi = Q\delta(\tau)$, where $\delta(\tau)$ is the *Kronecker* delta function [24], [25] and Q is the constant matrix. The variance matrix satisfies the equation $R_\eta(k+1) = GR_\eta(k)G^T + HQH^T$. When the constant k is large enough, $R_\eta(k)$ converges to the constant matrix, i.e.,

$$R_\eta = GR_\eta G^T + HQH^T. \tag{8}$$

The above equation is a Lyapunov function of a discrete-time system that demonstrates the relationship between the output sequence's variance R and filtering factor c_0. For *Fhan* algorithm, the matrices G and H are

$$G = \begin{pmatrix} 1 & h \\ \dfrac{1}{c_0 h} & 1 - \dfrac{2}{c_0} \end{pmatrix}, \quad H = \begin{pmatrix} 0 \\ \dfrac{1}{c_0^2 h} \end{pmatrix},$$

respectively. By assuming that the density of the white noise power spectrum is $Q = 1$, we achieve the results as shown in Fig. 2.

As demonstrated in Fig. 2, the TD can filter random noises when the proper filtering factor c_0 is selected. The proposed *Ftd* based TD performs better in filtering capacity than *Fhan* does.

B. PHASE DELAY COMPENSATION

From Fig. 1, we know that the phase delay will increase as the filtering factor c_0 increases. In this subsection, a phase delay compensation scheme, i.e., the TD group scheme, will be introduced to balance the trade-off between filtering quality and phase delay for better use in practice.

For a single TD, the filtering output is a function of filtering factor c_0, quickness factor r, time t, and time delay τ. Within a TD group, all TDs are connected in series, where the output of the former TD is the input of the latter one. By doing so, we improve the filtering quality compared with that of a single TD. However, for a single TD, there exists a time delay τ. For a TD group, the delay shall become longer. To solve this problem, we incorporate phase compensation into the TD group.

For a single TD, using Taylor's expansion to expand input signal $v(t-\tau)$ at time t, we obtain that

$$v(t-\tau) = v(t) + \dot{v}(t)(-\tau) + \frac{\ddot{v}(t)^2}{2!}(-\tau)^2 + \frac{\dddot{v}(t)^3}{3!}(-\tau)^3 + R(t,\tau), \tag{9}$$

where $R(t,\tau)$ is a higher-order error term.

Similarly, using Taylor's expansion, signal $v(t-i\tau)$ is expanded at time t, resulting in

$$v(t-i\tau) = v(t) - \dot{v}(t)(i\tau) + \frac{\ddot{v}(t)^2}{2!}(i\tau)^2 - \frac{\dddot{v}(t)^3}{3!}(i\tau)^3 + R(t,\tau). \tag{10}$$

Therefore, the relationship between input and output in the TD group is

$$\begin{cases} \bar{v}_1(t) = v(t-\tau) \\ \bar{v}_2(t) = v(t-2\tau) \\ \cdots \\ \bar{v}_m(t) = v(t-m\tau) \end{cases} \tag{11}$$

where m is the number of TDs within a TD group. Each equation in (11) can be expanded using Taylor's expansion. Ignoring all the higher-order terms, we obtain the final filtering output with phase compensation of the TD group as follows:

$$\bar{v} = \sum_{i=1}^{m} \alpha_{mi}\bar{v}_i \tag{12}$$

The candidates of the coefficient α_{mi} when m varies are presented in Table 1.

Theoretically, filtering quality improves as m increases. However, along with the increase of m, the computational burdens grow for the TD group. For real-world applications,

TABLE 1. The value of coefficient α_{mi}.

m	α_{m1}	α_{m2}	α_{m3}	α_{m4}	α_{m5}	α_{m6}	α_{m7}
2	2	-1					
3	3	-3	1				
4	4	-6	4	-1			
5	5	-10	10	-5	1		
6	6	-15	20	-15	6	-1	

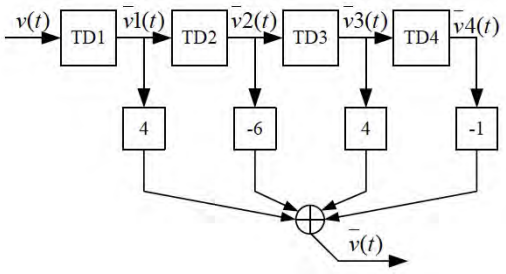

FIGURE 3. Block diagram of TD group with phase compensation when $m = 4$.

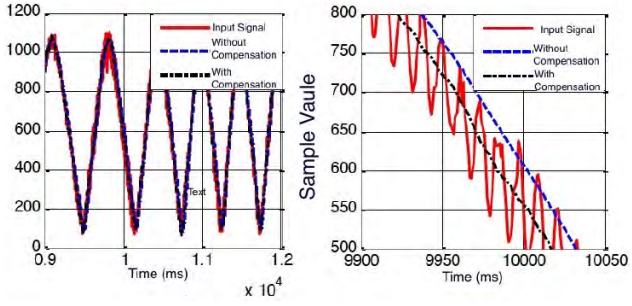

FIGURE 4. Filtering outputs and their partial enlargement with phase compensation for real data.

choosing the proper number of TDs shall balance the processing requirements for a system with the computational time needed. Figure 3 depicts the filtering output with phase compensation for real data when $m = 4$.

From Fig. 4, it can be observed that the filtering output of the TD group has a smaller phase delay and better filtering quality when phase compensation is included.

V. SIMULATION AND EXPERIMENT

A. COMPARISONS BY NUMERICAL SIMULATIONS

In this subsection, simulation results are presented to compare the *Ftd* algorithm based differentiator with the other four common differentiators. Specifically, we compare the errors of signal-tracking and differentiation acquisition among the following four different methods.

DI. Classic tracking differentiator based on two inertia elements [16].

$$\begin{cases} \dot{x}_1 = x_2, \\ \dot{x}_2 = -\dfrac{1}{\tau_1\tau_2}(x_1 - v) + \dfrac{\tau_1 + \tau_2}{\tau_1\tau_2}x_2 \end{cases}$$

DII. Sliding-mode technique based robust exact differentiator [10].

$$\begin{cases} \dot{x}_1 = x_2 - \alpha|x_1 - v|^{0.5}sign(x_1 - v), \\ \dot{x}_2 = -\beta sign(x_1 - v) \end{cases}$$

DIII. Tacking differentiator based on *Fhan* algorithm [16], [17].

$$\begin{cases} u(k) = Fhan(x_1(k) - v(k), x_2(k), r_0, c_0h), \\ x_1(k+1) = x_1(k) + hx_2(k), \\ x_2(k+1) = x_2(k) + hu(k), \quad |u(k)| \le r \end{cases}$$

DIV. The proposed tracking differentiator based on *Ftd* algorithm.

$$\begin{cases} u(k) = Ftd(x_1(k) - v(k), c_1x_2(k), r_0, c_0h), \\ x_1(k+1) = x_1(k) + hx_2(k), \\ x_2(k+1) = x_2(k) + u(k)h. \end{cases}$$

We use the Matlab program and the Euler method for this investigation. We generate the same input signal sequence $v(t) = \sin(0.25\pi t) + n(t)$, initial value $(x_{10} = 0.1, x_{20} = 1)$ and the sampling period $h = 0.001$ for all simulations. Therein the $n(t)$ is the random noise with the expression $n(t) = 0.1 \star rand(1)$ in Matlab code. The all relevant parameters are selected by means of trial and error. Specifically, for the classic differentiator **DI**, the parameters are $\tau_1 = 0.01$, $\tau_2 = 0.02$; for differentiator **DII**, the parameters are $\alpha = 1.5$, $\beta = 36$. For differentiator **DIII** and differentiator **DIV**, the damping factor is $c_1 = 2$ the quickness factor is $r_0 = 100$, the damping factor is $c_1 = 2$, and the filtering factor is $c_0 = 3$. The results from comparing errors of signal-tracking and differentiation acquisition among these four differentiators are demonstrated in Fig. 5 and Fig. 6. The average of absolute error (AAE) including tracking error (TE) and differentiation error (DE) for the four differentiators are presented in Table II.

According to the above results, we determine that, differentiators of **DIII** and **DIV** produce smaller errors both in signal tracking and differentiation acquisition, as the discontinuous function of **DII** produces a chattering problem and classic tracking differentiator **DI** based on two inertia elements would amplify the noise. What's more, the proposed differentiator **DIV** performs better in signal-tracking and differentiation acquisition than differentiator **DIII**.

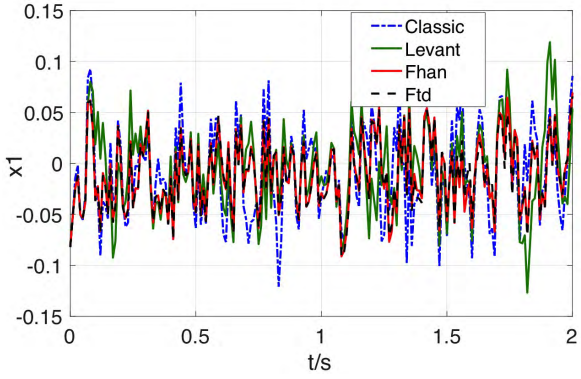

FIGURE 5. Comparisons of signal-tracking errors by four differentiators.

TABLE 2. The average of absolute error for the four differentiators.

Algorithm	AAE-TE	AAE-DE
DI	0.085	3.65
DII	0.074	2.12
DIII	0.056	1.83
DIV	0.048	1.54

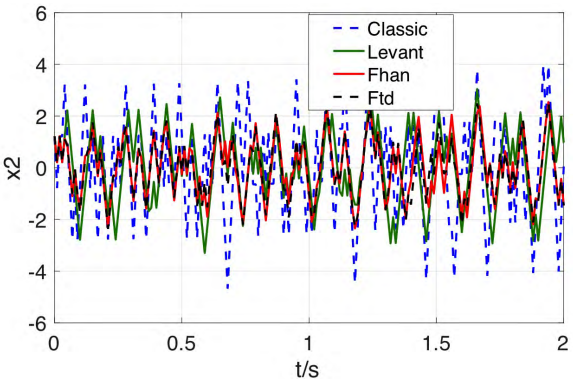

FIGURE 6. Comparisons of differentiation acquisition errors by four differentiators.

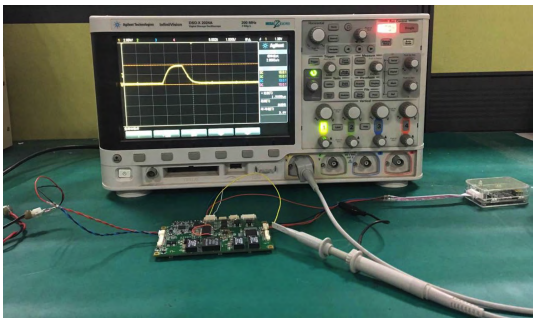

FIGURE 7. Experimental platform for calculating execution time using MCU (STM32F405).

TABLE 3. Comparisons of execution time among three algorithms.

Algorithm	Average real time execution
Levant	$5.45us$
Fhan	$5.25us$
Ftd	$3.15us$

B. COMPARISONS OF ALGORITHM EXECUTION TIME

We test how the proposed *Ftd* algorithm affects real-time execution. For this, the chip STM32F405 is adopted to compare the execution time needed for processing the same input signal by the three algorithms respectively (Fig. 7). In these experiments, the average execution time is calculated and presented in Table 3.

From such comparisons, we can observe that the proposed *Ftd* algorithm can help speed up real-time execution, which is beneficial for practical engineering applications.

VI. CONCLUSION

An efficient tracking differentiator (TD) based on a time criterion for the double integral systems is proposed. Under any given sampling period, the time-criterion based feedback control is presented to construct the TD. It relaxes the strict constraint on the sampling time for the discrete time optimal control (*Fhan*) based TD. The frequency domain analysis showed that the filtering factor is of high importance in signal-tracking filtering performance. Using the proposed TD group scheme can keep good balance between filtering quality and phase delay. The simulation results show that the proposed TD has advantages of smaller errors of signal tracking and differentiation extraction over existing common differentiators. Our experimental results showed that this new TD requires shortest real-time execution for processing the same input signals. Future work will include analyzing the convergence of the proposed *Ftd* algorithm and the stability of this TD.

APPENDIX A

In this appendix, we solve **Task 1** and **Task 2** in Section II in detail.

For **Task 1**, when $h \le t_A$, the control signal is $u = -s$; otherwise, that signal value should be decreased to guarantee that the state point $M(x_{10}, x_{20})$ can be driven to the switching curve Γ within the sampling time h. When the state point is located above the Γ, $s = +1$ and the control signal takes on $u = -u_a s$. u_a satisfies the following equations:

$$\begin{cases} x_1 = x_{10} - \dfrac{1}{2u_a}(x_2^2 - x_{20}^2) \\ x_2 = x_{20} - u_a h \end{cases} \tag{13}$$

Therefore, $x_1 = \frac{1}{2}x_2^2$ exists when the initial state point is driven back to the switch curve by the corresponding control signal sequence. If u_a is taken as being unknown, then

$$\frac{1}{2}h^2 u_a^2 + (\frac{1}{2}h^2 - hx_{20})u_a + \frac{1}{2}x_{20}^2 - x_{20}h - x_{10} = 0. \tag{14}$$

The discriminant of (14) is

$$\begin{aligned} \triangle &= (\frac{1}{2}h^2 - hx_{20})^2 - 2h^2(\frac{1}{2}x_{20}^2 - x_{20}h - x_{10}) \\ &= \frac{1}{4}h^4 + h^3 x_{20} + 2h^2 x_{10}. \end{aligned}$$

There are two possible cases as follows.

1) When $x_{20} \ge 0$, the discriminant satisfies the condition that

$$\begin{aligned} \triangle &> \frac{1}{4}h^4 + 2h^2(x_{10} + \frac{1}{2}x_{20}^2) \\ &= \frac{1}{4}h^4 + 2h^2(x_{10} + \frac{1}{2}x_{20}|x_{20}|) > \frac{1}{4}h^4 > 0; \end{aligned}$$

2) When $x_{20} < 0$, $x_{10} - \frac{1}{2}x_{20}^2 > 0$ can be derived because $x_{10} + \frac{1}{2}x_{20}|x_{20}| > 0$. Therefore,

$$\begin{aligned} \triangle &= \frac{1}{4}h^4 + h^3 x_{20} + 2h^2 x_{10} \\ &> \frac{1}{4}h^4 + h^3 x_{20} + 2h^2\frac{1}{2}x_{20}^2 = h^2(x_{20} + \frac{1}{2}h)^2 \ge 0. \end{aligned}$$

For these two cases, the discriminant can always satisfy $\bigtriangleup > 0$. Furthermore, two unequal real roots can satisfy $x_2(h) < 0$. Because $x_2(h) = x_{20} - u_a h = \frac{h}{2} \pm \frac{\sqrt{\bigtriangleup}}{h} < 0$,

the positive root is excluded and the expression of u_a is obtained as follows:

$$u_a = -\frac{1}{2} + \frac{1}{h}x_{20} + \frac{1}{2}\sqrt{1 + \frac{4}{h}x_{20} + \frac{8}{h^2}x_{10}}. \quad (15)$$

Similarly, when state point M is located below Γ, $s = -1$ and the control input is $u = u_a s$. It can be derived that

$$u_a = -\frac{1}{2} - \frac{1}{h}x_{20} + \frac{1}{2}\sqrt{1 - \frac{4}{h}x_{20} - \frac{8}{h^2}x_{10}}. \quad (16)$$

To sum up, the resulting expression of u_a when state point M is located above or below Γ is

$$u_a = -\frac{1}{2} - \frac{s}{h}x_{20} + \frac{1}{2}\sqrt{1 + (\frac{4}{h}x_{20} - \frac{8}{h^2}x_{10})s} \quad (17)$$

where parameter s has the same definition as described in the previous section.

For **Task 2**, when state point M is located on the switching curve Γ, i.e., $\Gamma(x_{10}, x_{20}) = 0$. Without loss of generality, we consider the state point M as being in the fourth quadrant, then it satisfies $x_1(t) = \frac{1}{2}x_2^2(t)$. When $h \leq t_B$ ($t_B = |x_{20}|$), the control law is $u = -sign(x_{20})$. However, when $h > t_B$, the control signal value should be decreased to guarantee that state point M can be driven back to the origin. In order to drive the state point M back to the origin within only one step, the control signal must satisfy the following condition:

$$\begin{cases} x_1(t) = x_{10} + x_{20}t + \int_0^t \int_0^\tau u(\sigma)d\sigma d\tau = 0 \\ x_2(t) = x_{20} + \int_0^t u(\tau)d\tau = 0. \end{cases} \quad (18)$$

where $t = h$. For simplicity, we suppose $u = a + bt$ ($t = h$) and substitute it into (18). Thus we have

$$\begin{cases} x_{20} + ah + \frac{1}{2}bh^2 = 0 \\ x_{10} + x_{20}h + \frac{1}{2}ah^2 + \frac{1}{6}bh^3 = 0, \end{cases} \quad (19)$$

which leads to

$$\begin{cases} a = -\frac{2}{h^2}(2x_{20})h + 3x_{10}) \\ b = \frac{6}{h^3}(x_{20})h + 2x_{10}). \end{cases} \quad (20)$$

APPENDIX B

In this appendix, we present the proof of *Theorem 1*. We split the proof into two steps according to the initial condition of $x_2(0)$ when $x_{20} \geq 0$ $x_{20} < 0$, respectively.

Step 1: When $x_{20} \geq 0$ (note that $x_{20} < h$ and $x_{10} < h^2$ because $t_A = x_{20} + \sqrt{x_{10} + \frac{1}{2}x_{20}^2} < h$), since

$$\begin{aligned} h(x_{20} + \frac{2}{h}x_{10}) &= hx_{20} + 2x_{10} \\ &> x_{20}^2 + 2x_{10} = 2(\frac{1}{2}x_{20}^2 + x_{10}) > 0 \end{aligned}$$

and $u_a > \frac{1}{h}x_{20} \geq 0$, $u_a^2 < 1$ is derived by proving $u_a < 1$. The followings are equivalent inequalities:

$$\begin{aligned} u_a < 1 &\Leftrightarrow \\ (\frac{3}{2} - \frac{1}{h}x_{20})^2 > \frac{1}{4}(1 + \frac{4}{h}x_{20} + \frac{8}{h^2}x_{10}) &\Leftrightarrow \\ 2(1 - \frac{1}{h^2}x_{10}) > 0 > \frac{4}{h}x_{20} - \frac{1}{h}x_{20}^2 - \frac{1}{h^2}x_{20}^2 &\Leftrightarrow \\ x_{10} < h^2, x_{20} < 4h. \end{aligned}$$

The above inequalities hold because $x_{20} < h, x_{10} < h^2$.

Step 2: When $x_{20} < 0$,

$$x_{10} + \frac{1}{2}x_{20}|x_{20}| > 0, \quad x_{10} - \frac{1}{2}x_{20}^2 > 0.$$

Thus, we have

$$u_a > -\frac{1}{2} + \frac{x_{20}}{h} + |\frac{1}{2} + \frac{x_{20}}{h}| > -1.$$

The final step is to prove $u_a < 1$ and demonstrate the existence of equivalent inequalities. We have

$$\begin{aligned} u_a < 1 &\Leftrightarrow \\ 3 - \frac{2}{h}x_{20} > \sqrt{1 + \frac{4}{h}x_{20} + \frac{8}{h^2}x_{10}} &\Leftrightarrow \\ 2 + \frac{1}{h^2}x_{20}^2 > \frac{4}{h}x_{20} + \frac{2}{h^2}x_{10}. \end{aligned}$$

Because $t_A < h, x_{10} < \frac{1}{2}x_{20}^2 + h^2 + 2|x_{20}|h$, we have $\frac{1}{2}x_{20}^2 < x_{10} < \frac{1}{2}x_{20}^2 + h^2 + 2|x_{20}|h$. Substituting the inequality into the last equivalent inequality above, we can derive that

$$\begin{aligned} \frac{4}{h}x_{20} + \frac{2}{h^2}x_{10} &< \frac{4}{h}x_{20} + \frac{2}{h^2}(\frac{1}{2}x_{20}^2 + h^2 + 2|x_{20}|h) \\ &= 2 + \frac{1}{h^2}x_{20}^2 + \frac{4}{h}(x_{20} + |x_{20}|) = 2 + \frac{1}{h^2}x_{20}^2. \end{aligned}$$

Thus, $\frac{4}{h}x_{20} + \frac{2}{h^2}x_{10} < 2 + \frac{1}{h^2}x_{20}^2$, which always satisfies $|u_a| < 1$.

For a general discrete-time double-integral system, its control signal sequence is obtained by substituting the x_1 and x_2 with z_1 and z_2 respectively, where $z_1 = \frac{x_1}{r}$ and $z_2 = \frac{x_2}{r}$. Deriving u_a easily satisfies the condition $|u_a| < r$ and the proof is completed.

ACKNOWLEDGMENT

This work was supported in part by the National Research Foundation of Singapore (NRF) under its Campus for Research Excellence and Technological Enterprise (CREATE) program, in part by the Ministry of Education (MOE), Singapore, under Contract MOE 2016-T2-1-119, in part by the Interdisciplinary Graduate School, Nanyang Technological University, Singapore, and in part by the National Key Research and Development Program of China under Grant 2016YFB1200600.

REFERENCES

[1] K. H. Ang, G. Chong, and Y. Li, "PID control system analysis, design, and technology," *IEEE Trans. Control Syst. Technol.*, vol. 13, no. 4, pp. 559–576, Jul. 2005.
[2] A. Oustaloup, F. Levron, B. Mathieu, and F. M. Nanot, "Frequency-band complex noninteger differentiator: Characterization and synthesis," *IEEE Trans. Circuits Syst. I, Fundam. Theory Appl.*, vol. 47, no. 1, pp. 25–39, Jan. 2000.
[3] Y. Li, K. H. Ang, and G. C. Y. Chong, "PID control system analysis and design," *IEEE Control Syst.*, vol. 26, no. 1, pp. 32–41, Feb. 2006.
[4] K. Lu, W. Zhou, G. Zeng, and W. Du, "Design of PID controller based on a self-adaptive state-space predictive functional control using extremal optimization method," *J. Franklin Inst.*, vol. 355, no. 5, pp. 2197–2220, Mar. 2018.
[5] L. Sun, D. Li, and K. Y. Lee, "Enhanced decentralized PI control for fluidized bed combustor via advanced disturbance observer," *Control Eng. Pract.*, vol. 42, pp. 128–139, Sep. 2015.
[6] G. Silva, A. Datta, and S. P. Bhattacharyya, "PI stabilization of first-order systems with time delay," *Automatica*, vol. 37, no. 12, pp. 2025–2031, Dec. 2001.
[7] F. Deza, E. Busvelle, J. P. Gauthier, and D. Rakotopara, "High gain estimation for nonlinear systems," *Syst. Control Lett.*, vol. 18, no. 4, pp. 295–299, Apr. 1992.
[8] S. Ibrir, "Linear time-derivative trackers," *Automatica*, vol. 40, no. 3, pp. 397–405, 2004.
[9] T. Gonzalez, J. A. Moreno, and L. Fridman, "Variable gain super-twisting sliding mode control," *IEEE Trans. Autom. Control*, vol. 57, no. 8, pp. 2100–2105, Aug. 2013.
[10] A. Levant, "Robust exact differentiation via sliding mode technique," *Automatica*, vol. 34, no. 3, pp. 379–384, Mar. 1998.
[11] A. Levant, "Non-homogeneous finite-time-convergent differentiator," in *Proc. 48th IEEE Conf. CDC/CCC*, Dec. 2009, pp. 8399–8404.
[12] X. Wang, Z. Chen, and G. Yang, "Finite-time-convergent differentiator based on singular perturbation technique," *IEEE Trans. Autom. Control*, vol. 52, no. 9, pp. 1731–1737, Sep. 2007.
[13] H. Alwi and C. Edwards, "An adaptive sliding mode differentiator for actuator oscillatory failure case reconstruction," *Automatica*, vol. 49, no. 2, pp. 642–651, 2013.
[14] A. Polyakov, D. Efimov, and W. Perruquetti, "Homogeneous differentiator design using implicit Lyapunov Function method," in *Proc. IEEE Eur. Control Conf.*, Jun. 2014, pp. 288–293.
[15] Y. Shtessel, C. Edwards, L. Fridman, and A. Levant, "Higher-order sliding mode controllers and differentiators," *Sliding Mode Control Observation*. New York, NY, USA: Springer, 2014.
[16] J. Han, "From PID to active disturbance rejection control," *IEEE Trans. Ind. Electron.*, vol. 56, no. 3, pp. 1731–1737, Mar. 2009.
[17] H. Zhang, Y. Xie, G. Xiao, and C. Zhai, "Closed-form solution of discrete-time optimal control and its convergence," *IET Control Theory Appl.*, vol. 12, no. 3, pp. 413–418, Feb. 2017.
[18] B. Guo and Z. Zhao, *Active Disturbance Rejection Control for Nonlinear Systems: An Introduction*. Hoboken, NJ, USA: Wiley, 2016.
[19] J. Li, Y. Xia, X. Qi, and Z. Gao, "On the necessity, scheme, and basis of the linear–nonlinear switching in active disturbance rejection control," *IEEE Trans. Ind. Electron.*, vol. 64, no. 2, pp. 1425–1435, Feb. 2017.
[20] J. Han, "Nonlinear PID controller," *Acta Automatica Sinica*, vol. 20, no. 4, pp. 487–490, Feb. 1994.
[21] H. Zhang, Y. Xie, G. Xiao, C. Zhai, and Z. Long, "A simple discrete-time tracking differentiator and its application to speed and position detection system for a maglev train," *IEEE Trans. Control Syst. Technol.*, vol. 27, no. 4, pp. 1728–1734, Jul. 2019.
[22] F. Lin, *Robust Control Design: Optimazation Control Approach*, vol. 18. Hoboken, NJ, USA: Wiley, 2007.
[23] A. Krener, "A generalization of Chow's theorem and the bang-bang theorem to nonlinear control problems," *SIAM J. Control Optim.*, vol. 12, no. 1, pp. 43–52, Feb. 1974.
[24] M. Fontana and K. Loper, "Kronecker function rings: a general approach," in *Lecture Notes in Pure and Applied Mathematics*, 2001, pp. 189–206.
[25] A. M. Zoubir and B. Boashash, "The bootstrap and its application in signal processing," *IEEE Signal Process. Mag.*, vol. 15, no. 1, pp. 56–76, Jan. 1998.
[26] A. Accetta, M. Cirrincione, M. Pucci, and G. Vitale, "Sensorless control of PMSM fractional horsepower drives by signal injection and neural adaptive-band filtering," *IEEE Trans. Ind. Electron.*, vol. 59, no. 3, pp. 1355–1366, Mar. 2012.
[27] T. Laczynski and A. Mertens, "Predictive stator current control for medium voltage drives with LC filters," *IEEE Trans. Power Electron.*, vol. 24, no. 11, pp. 2427–2435, Nov. 2009.
[28] M. Barut, S. Bogosyan, and M. Gokasan, "Speed-sensorless estimation for induction motors using extended Kalman filters," *IEEE Trans. Ind. Electron.*, vol. 54, no. 1, pp. 272–280, Feb. 2007.

YUNDE XIE received the Ph.D. degree in control science and control engineering from the National University of Defense Technology, China, in 1998, where he was an Associate Professor, in 2004. He is currently a Senior Engineer with Beijing Maglev Transportation Development Company Ltd. His research interests include nonlinear control theory and application, and maglev control techniques.

HEHONG ZHANG is currently pursuing the Ph.D. degree with the Interdisciplinary Graduate School, Nanyang Technological University, Singapore. He is also with the Future Resilient Systems, Singapore-ETH Centre. His research interests include signal processing, theory and application of optimal control and nonlinear control theory, and particularly time optimal control-based tracking differentiator.

LONGHUA SHE received the Ph.D. degree in control science and control engineering from the National University of Defense Technology, China, in 1998, where he was a Full Professor, in 2010. He is currently a Senior Engineer with Beijing Maglev Transportation Development Company Ltd. His research interest includes maglev control techniques, particularly disturbance rejection control and suspension control for maglev train.

GAOXI XIAO (SM'19) received the B.S. and M.S. degrees in applied mathematics from Xidian University, Xi'an, China, in 1991 and 1994, respectively, and the Ph.D. degree in computing from Hong Kong Polytechnic University, in 1998. He was an Assistant Lecturer with Xidian University, from 1994 to 1995. He was a Postdoctoral Research Fellow with Polytechnic University, Brooklyn, NY, USA, in 1999, and a Visiting Scientist with the University of Texas at Dallas, from 1999 to 2001. He joined the School of Electrical and Electronic Engineering, Nanyang Technological University, Singapore, in 2001, where he is currently an Associate Professor. His research interests include complex systems and complex networks, communication networks, smart grids, and system resilience and risk management. He serves/served as an Associate Editor or a Guest Editor for the IEEE TRANSACTIONS ON NETWORK SCIENCE AND ENGINEERING, *PLOS ONE*, and *Advances in Complex Systems*. He is a TPC member for numerous conferences, including the IEEE ICC and the IEEE GLOBECOM.

CHAO ZHAI (M'13) received the B.E. degree in automation engineering from Henan University, Kaifeng, China, in 2007, the M.E. degree in control science and engineering from the Huazhong University of Science and Technology, Wuhan, China, in 2009, and the Ph.D. degree in complex system and control from the Institute of Systems Science, Chinese Academy of Sciences, Beijing, China, in 2013. From July 2013 to August 2015, he was a Postdoctoral Fellow with the University of Bristol, U.K. He is currently a Research Fellow with the Singapore-ETH Centre, Singapore. His research interests include optimal control, signal processing, cascading failure in power systems, and evolutionary game theory.

TSO-CHIEN PAN received the B.S. degree from the National Cheng Kung University, Taiwan, and the Ph.D. and M.S. degrees from the University of California at Berkeley, USA. He joined NTU faculty, in 1985, and served for five years as the NTU Dean of the College of Engineering before taking on the leadership of ICRM at NTU, in 2011. He is the Founding Executive Director of the Institute of Catastrophe Risk Management (ICRM), Nanyang Technological University (NTU), Singapore. He is currently leading the national Research and Development effort on Natural Catastrophe Data Analytics Exchange Project, a Singapore initiative of public-private partnership for the Southeast Asia region. He specializes in the analysis and design of structures against earthquake ground motions and other forms of dynamic loading, and he has been working on natural catastrophe risk assessment of major urban centers. He has made important contributions to both national and international research communities. He has served for a long period as the Secretary General of the World Seismic Safety Initiative, International Association for Earthquake Engineering. He is also a Fellow of the Academy of Engineering, Singapore, and a Fellow of the ASEAN Academy of Engineering and Technology.